

# A Riemannian Framework for the Processing of Tensor-Valued Images

Pierre Fillard, Vincent Arsigny, Nicholas Ayache, and Xavier Pennec

INRIA Sophia Antipolis - Epidaure Project,  
2004 Route des Lucioles BP 93,  
06902 Sophia Antipolis Cedex, France  
{Pierre.Fillard, Vincent.Arsigny, Nicholas.Ayache,  
Xavier.Pennec}@Sophia.Inria.fr

**Abstract.** In this paper, we present a novel framework to carry out computations on tensors, i.e. symmetric positive definite matrices. We endow the space of tensors with an affine-invariant Riemannian metric, which leads to strong theoretical properties: The space of positive definite symmetric matrices is replaced by a regular and geodesically complete manifold without boundaries. Thus, tensors with non-positive eigenvalues are at an infinite distance of any positive definite matrix. Moreover, the tools of differential geometry apply and we generalize to tensors numerous algorithms that were reserved to vector spaces. The application of this framework to the processing of diffusion tensor images shows very promising results. We apply this framework to the processing of structure tensor images and show that it could help to extract low-level features thanks to the affine-invariance of our metric. However, the same affine-invariance causes the whole framework to be noise sensitive and we believe that the choice of a more adapted metric could significantly improve the robustness of the result.

## 1 Introduction

Symmetric positive definite matrices, or tensors, are widely used in image processing. They can either characterize the diffusion of water molecules as in diffusion tensor imaging (DTI) [1], or reveal structural information of an image (structure tensor) [2, 3]. In this last application, tensors are used to detect singularities such as edges or corners in images. The structure tensor is classically obtained by a Gaussian smoothing of the tensor product of the gradient, or with a non-linear filtering as in [4], thus being naturally robust to noise. However, noisy images require a large amount of regularization to obtain a smooth structure tensor field in order to avoid being overwhelmed by outliers in features detection. By contrast, too much smoothing would completely wipe out small structures in images. To address this problem, one would prefer to preserve small structures in images by estimating structure tensors with a little smoothing and to regularize the noisy tensor field itself. This implies to be able to filter tensor images, and more generally to carry out computations with tensors.

Working with tensors is arduous since the underlying space is a manifold that is not a vector space. While convex operations remain stable on the tensor space (e.g. the mean of a set of tensors is a tensor), one can quickly go out of the Euclidean boundaries with non-convex operations like a gradient descent. A critical consequence is that matrices with null or negative eigenvalues may appear and are problematic for most applications.

In this paper, we propose to apply a recently proposed Riemannian framework for tensors to the processing of structure tensor images. The limitations of the standard Euclidean calculus are completely overcome and the tensor space is replaced by a manifold with a regular structure. We show that it leads to very strong theoretical properties, such as the existence and uniqueness of the mean, and that most of the statistical tools as well as the algorithms that were until now reserved to vector space can be extended to tensors. The rest of the paper is organized as follows. In Sec. 2 we summarize the Riemannian framework for tensors. In Sec. 3, we extend the computations of classical image processing operators to tensors as well as more complex operations and we provide intrinsic numerical schemes for their implementation. In Sec. 4, we apply these tools on a structure tensor image. In particular, we perform an anisotropic smoothing and discuss about the potentiality of the method on this type of tensors.

## 2 A Riemannian Framework for Tensor Calculus

Much of the literature addresses tensor computing problems in the context of DTI regularization. In DTI, the Brownian motion of water is estimated by a MRI scanner at each position of the brain. This stochastic motion is characterized by its covariance matrix, which is called a diffusion tensor. Depending on the amount and direction of water diffusion, the tensor can be either cigar-shaped (region where the diffusion is restricted by oriented tissues), or a sphere (regions with free diffusion). As the MRI signal is corrupted with noise during acquisition, the resulting tensor field has to be filtered. To do so, the spectral decomposition of tensors is often exploited: [5] only processes the major eigenvector (eigenvector corresponding to the largest eigenvalue), leading to simple computations but a dramatical loss of information, while [6] independently regularizes the orthogonal matrices of eigenvectors and the eigenvalues. As the spectral decomposition is not unique, a preprocess step, where the eigenvectors are reoriented, is needed and is not trivial. More recently, differential geometric approaches have been developed to generalize the PCA to tensor data [7], for statistical segmentation of tensor images [8], for computing a geometric mean and an intrinsic anisotropy index [9], or as the basis of a full framework for Riemannian tensor calculus [10]. In this last work, we endow the space of tensors with an affine-invariant Riemannian metric to obtain results that are independent of the choice of the spatial coordinate system. Differential geometry tools allow to manipulate tensors while insuring the positive definiteness of the result. In this section, we present an overview of the affine-invariant metric for tensors.

## 2.1 An Affine-Invariant Riemannian Metric

We showed in [11] that choosing a Riemannian metric provides a powerful framework to generalize statistics and other operations to manifolds. We applied this concept to tensors and showed in [10] that it leads to interesting properties such as the existence and uniqueness of the (geometric) mean or the existence and uniqueness of the geodesic between two tensors. A complete description of the features of this framework can be found in [10] and is summarized below.

Let  $\Sigma$  be a point of the tensor space  $Sym_+^*(n)$ . The action of the linear group  $GL_n$  on  $Sym_+^*(n)$  is:

$$\forall A \in GL_n, A \star \Sigma = A \Sigma A^T$$

Let us consider the standard matrix scalar product at the tangent space at identity  $T_{I_d}M$ :

$$\langle W_1 | W_2 \rangle_{I_d} \stackrel{def}{=} \text{Tr}(W_1 W_2^T),$$

where  $W_1$  and  $W_2$  are elements of  $T_{I_d}M$ . As tangent spaces are vectorial spaces,  $W_1$  and  $W_2$  are called tangent vectors. They are simple symmetric matrix since the tensor space is a manifold included in the space of symmetric matrices  $Sym(n)$ .

An affine-invariant metric must verify:  $\langle W_1 | W_2 \rangle_\Sigma = \langle A \star W_1 | A \star W_2 \rangle_{A \star \Sigma}$  for all  $A \in GL_n$ . This is verified in particular for  $A = \Sigma^{-1/2}$ , which allows us to write the scalar product at any point  $\Sigma$  from the product at  $T_{I_d}M$ :

$$\langle W_1 | W_2 \rangle_\Sigma = \left\langle \Sigma^{-\frac{1}{2}} \star W_1 | \Sigma^{-\frac{1}{2}} \star W_2 \right\rangle_{I_d} \quad (1)$$

$$= \text{Tr} \left( \Sigma^{-\frac{1}{2}} W_1 \Sigma^{-1} W_2 \Sigma^{-\frac{1}{2}} \right) \quad (2)$$

Eq. 1 is an affine-invariant Riemannian metric. Actually, we only need the invariance by the linear group to obtain an affine-invariance since the translation is not taken into account in our applications (tensors are independent of their position on a grid).

As a general property on Riemannian manifolds, geodesics realize a local diffeomorphism, called the exponential map, from the tangent space at any point  $\Sigma$  to the manifold itself. This allows us to locally identify points of the manifold with tangent vectors. With the invariant metric of Eq. 1, we can show that this diffeomorphism is moreover global and is simply expressed with the matrix exponential:

$$\forall W \in T_\Sigma M, \quad \exp_\Sigma(W) = \Sigma^{\frac{1}{2}} \exp \left( \Sigma^{-\frac{1}{2}} W \Sigma^{-\frac{1}{2}} \right) \Sigma^{\frac{1}{2}} \quad (3)$$

$\exp_\Sigma(W)$  can be seen as the point of the manifold reached by the geodesic starting at  $\Sigma$ , with tangent vector  $W$  in a unit time step. Conversely, we can uniquely define the inverse mapping, the logarithmic map:

$$\log_\Sigma(A) = \Sigma^{\frac{1}{2}} \log \left( \Sigma^{-\frac{1}{2}} A \Sigma^{-\frac{1}{2}} \right) \Sigma^{\frac{1}{2}}. \quad (4)$$

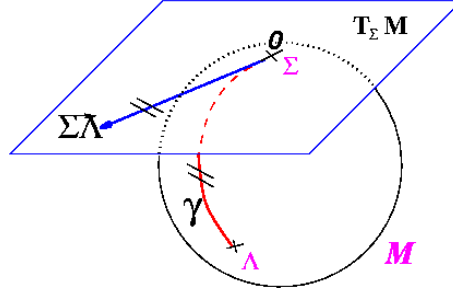


**Fig. 1. Development of the geodesic  $\gamma$  linking  $\Sigma$  to  $\Lambda$  onto the tangent space  $T_\Sigma M$ .** The geodesics starting at  $\Sigma$  are straight lines in  $T_\Sigma M$  and the distance along them is conserved.

These diffeomorphisms turn any two points  $\Sigma$  and  $\Lambda$  of the manifold into the tangent vector  $\overrightarrow{\Sigma\Lambda}$  such that the geodesic starting at  $\Sigma$  and with tangent vector  $\overrightarrow{\Sigma\Lambda}$  reaches the point  $\Lambda$  in a unit step (Fig. 1).

These two diffeomorphisms are the key to the numerical implementation and generalization to manifolds of numerous algorithms that work on a vector space. Table 1 summarizes the basic operations of vector spaces and their Riemannian counterparts.

*Geodesic marching:* An important operator for solving partial differential equations (PDEs) is the gradient descent. It consists in following the opposite direction of the gradient of a criterion  $C$  we want to minimize for a short time step  $\varepsilon$ . In the tensor case, the Euclidean gradient descent scheme  $\Sigma_{t+1} = \Sigma_t - \varepsilon \nabla C$  could easily lead out of the boundaries of the space and non-positive matrices may appear. The Euclidean scheme is advantageously replaced by the *geodesic marching scheme*: we follow the geodesic starting at  $\Sigma_t$ , with tangent vector  $-\nabla C$  for a short time step:  $\Sigma_{t+1} = \exp_{\Sigma_t}(-\varepsilon \nabla C)$ . The exponential map insures that we always stay on the manifold: the result is guaranteed to be positive definite.

Operation	Vector space	Riemannian manifold
Subtraction	$\overrightarrow{\Sigma\Lambda} = \Lambda - \Sigma$	$\overrightarrow{\Sigma\Lambda} = \log_\Sigma(\Lambda)$
Addition	$\Lambda = \Sigma + \overrightarrow{\Sigma\Lambda}$	$\Lambda = \exp_\Sigma(\overrightarrow{\Sigma\Lambda})$
Distance	$dist(\Sigma, \Lambda) = \ \overrightarrow{\Sigma\Lambda}\ $	$dist(\Sigma, \Lambda) = \ \overrightarrow{\Sigma\Lambda}\ _\Sigma$
Mean value	$\sum_i \overrightarrow{\Sigma\Sigma_i} = 0$	$\sum_i \log_\Sigma(\Sigma_i) = 0$
Gradient descent	$\Sigma_{t+\varepsilon} = \Sigma_t - \varepsilon \nabla C(\Sigma_t)$	$\Sigma_{t+\varepsilon} = \exp_{\Sigma_t}(-\varepsilon \nabla C(\Sigma_t))$
Linear (geodesic) interpolation	$\Sigma(t) = \Sigma_1 + t \overrightarrow{\Sigma_1\Sigma_2}$	$\Sigma(t) = \exp_{\Sigma_1}(t \overrightarrow{\Sigma_1\Sigma_2})$

**Table 1.** Re-interpretation of the basic operations of vector spaces to Riemannian manifolds.

In conclusion, the Riemannian framework gives a powerful alternative to the standard Euclidean calculus: classical operators are easily translated to tensors thanks to the combination of the logarithm and exponential maps and complex algorithms can be rewritten using these two diffeomorphisms. In the next section, we show that the classical image processing operators like gradient and Laplacian can be adapted to the Riemannian framework without much effort. More interestingly, we are able to achieve complex operations like anisotropic filtering directly on tensors, which was not possible with the standard Euclidean calculus.

### 3 Applications

In this section, we reinterpret various image processing operators in the Riemannian framework. First, we rewrite two classical operators of image processing (gradient and Laplacian) to tensor images, and second we describe more complex operations like multi-linear interpolation and anisotropic filtering.

#### 3.1 Classical Image Processing Operators

In the following, we show that the gradient and Laplacian of a tensor field are easily expressed in our exponential chart, and we provide a practical numerical implementation of both operators.

**Spatial Gradient of a Tensor Field** Basically, for a  $n$ -dimensional vector field  $F(x)$  defined over  $\mathbb{R}^d$ , the spatial gradient in an orthonormal basis is:  $\nabla F = [\partial_{x_1} F, \dots, \partial_{x_d} F]^T$ , where  $\partial_{x_i} F$  is the directional derivative of  $F$  in the direction  $x_i$ . It can be approximated using a finite difference scheme:  $\partial_{x_i} F(x) = (F(x + x_i) - F(x - x_i)) / (2\|x_i\|)$ .

For a tensor-valued image  $\Sigma(x)$ , we can proceed similarly except that the directional derivatives  $\partial_{x_i} \Sigma$  are now tangent vectors of  $T_{\Sigma(x)}M$ . They can be approximated like above using finite differences in our exponential chart:

$$\begin{aligned} \partial_{x_i} \Sigma(x) &\simeq \left( \overrightarrow{\Sigma(x)\Sigma(x+x_i)} - \overrightarrow{\Sigma(x)\Sigma(x-x_i)} \right) / (2\|x_i\|) \\ &= \left( \log_{\Sigma(x)}(\Sigma(x+x_i)) - \log_{\Sigma(x)}(\Sigma(x-x_i)) \right) / (2\|x_i\|). \end{aligned}$$

One must be careful to take the metric at point  $\Sigma(x)$  into account when computing the norm of the gradient:  $\|\nabla \Sigma(x)\|_{\Sigma(x)}^2 = \sum_{i=1}^d \|\partial_{x_i} \Sigma(x)\|_{\Sigma(x)}^2$ . Fig. 2 shows the difference between the Euclidean and Riemannian gradients. The Euclidean gradient (Fig. 2 middle) gives much more importance to tensors with large coefficients, and consequently its norm has higher values along the boundaries with the ventricles (a region characterized by large tensors), and lower values elsewhere. By contrast, the affine-invariant metric (Fig. 2 right) gives as much importance to variations of small tensors as to variations of large matrices. Consequently, the norm the Riemannian gradient is more regular.

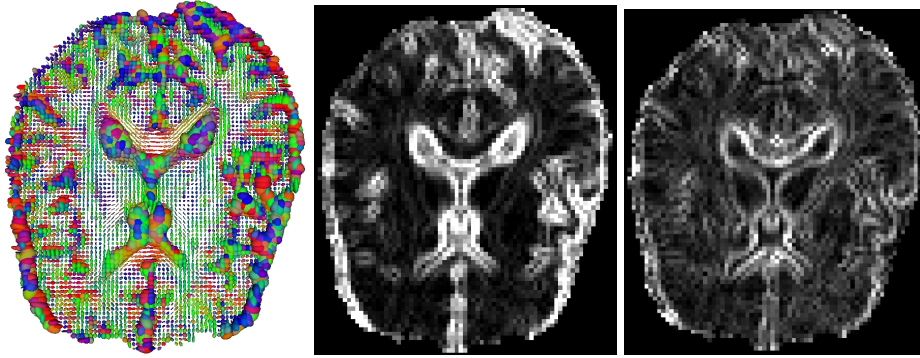


**Fig. 2.** Comparison of the norm of the Euclidean and Riemannian gradients of a tensor image. **Left:** A slice of a DTI tensor image. The color codes for the major eigenvectors of tensors: **Red:** left-right oriented tensor, **blue:** inferior-superior oriented tensor, **green:** posterior-anterior oriented tensor. **Middle:** Norm of the Euclidean gradient. **Right:** Norm of the Riemannian gradient. Remark how the Riemannian norm is more regular than the Euclidean norm.

**Laplacian of a Tensor Field** For the numerical implementation of the Laplacian, one needs the second order derivatives. As for the gradient, we use the finite difference scheme to approximate the 2nd order derivative on a discrete grid:  $\partial_{x_i}^2 F(x) \simeq (F(x + x_i) - 2F(x) + F(x - x_i)) / \|x_i\|^2$ . We proved in [10] that :

$$\partial_{x_i}^2 \Sigma(x) = \left( \overrightarrow{\Sigma(x)\Sigma(x + x_i)} + \overrightarrow{\Sigma(x)\Sigma(x - x_i)} \right) / \|x_i\|^2$$

is a forth order approximation of the  $2^{nd}$  order directional derivative of  $\Sigma(x)$  in the direction  $x_i$ . Finally, the manifold Laplacian (Laplace-Beltrami operator) of a tensor field is simply:  $\Delta \Sigma(x) = \sum_{i=1}^d \partial_{x_i}^2 \Sigma(x)$ .

### 3.2 Interpolation and Filtering of Tensor Fields

**Interpolation** Interpolation is one of the most important task in image processing. A simple operation is the interpolation between two tensors  $\Sigma_1$  and  $\Sigma_2$ . The classical Euclidean calculus gives us the formulation:  $\Sigma(t) = (1-t)\Sigma_1 + t\Sigma_2$ . With our Riemannian framework, it consists in following the geodesic joining the two tensors:  $\Sigma(t) = \exp_{\Sigma_1}(t\overrightarrow{\Sigma_1\Sigma_2})$ .

For multi-linear interpolation, e.g. bi or trilinear interpolation on a regular 2D or 3D grid, the formulation is not trivial. One has to go through the computation of a weighted mean with classical bi- or trilinear coefficients calculated on a grid. With the standard Euclidean framework, the weighted mean of a set of tensors is:  $\Sigma = (\sum_{i=1}^N \omega_i \Sigma_i) / \sum_{i=1}^N \omega_i$ . In our Riemannian framework, one needs to go

back to the Frechet definition of the mean, i.e. the minimum (if it exists) of the square distance to each tensor:

$$\bar{\Sigma} = \min_{\Sigma} \sum_{i=1}^N \text{dist}^2(\Sigma, \Sigma_i)$$

In the case of the tensor space provided with the affine-invariant metric, the manifold has a non-positive curvature, so that the mean exists and is unique. However, because of the curvature, the Frechet formulation does not have an explicit solution. Instead, one has to minimize it through a Newton gradient descent and the estimation of the mean at time  $t + 1$  is given by:

$$\bar{\Sigma}_{t+1} = \exp_{\bar{\Sigma}_t} \left( \frac{\sum_{i=1}^N \omega_i \log_{\bar{\Sigma}_t}(\Sigma_i)}{\sum_{i=1}^N \omega_i} \right)$$

which consists in expressing each tensor in the tangent space at the current estimation of the mean with the logarithmic map, then going back to the manifold with the exponential map, and to reiterate the process. The existence and uniqueness of the mean guarantees the process to converge. In practice, the convergence of the iterative process is geometric and the mean value is reached after 5 to 10 iterations. In [10], we propose an extension of several statistical operations to tensors.

**Anisotropic Filtering** In practice, we would like to filter a tensor image within homogeneous regions but not across the boundaries. The basic idea introduced by [12] is to penalize the smoothing in the directions where the magnitude of the gradient is high. This can be achieved through the minimization of the  $\phi$ -functional:

$$C(\Sigma) = \frac{1}{2} \int_{\Omega} \phi(\|\nabla \Sigma(x)\|_{\Sigma(x)}) dx. \quad (5)$$

By choosing an adequate  $\phi$ -function, one can give to the regularization an isotropic or anisotropic behavior [13]. In our experiments, we use  $\phi(s) = 2\sqrt{1 + s^2/\kappa^2} - 2$ , as proposed in [5]. The main difference with a classical Euclidean calculation is that we have to take the curvature into account by using the Laplace-Beltrami operator, and by expressing directional derivatives in the correct tangent space. After differentiation of Eq. 5, one obtains :

$$\nabla C(\Sigma) = -\frac{\phi(\|\nabla \Sigma\|_{\Sigma(x)})}{\|\nabla \Sigma\|_{\Sigma(x)}} \Delta \Sigma - \sum_{i=1}^d \partial_{x_i} \phi(\|\nabla \Sigma\|_{\Sigma(x)}) \partial_{x_i} \Sigma$$

Thanks to the numerical scheme of the gradient and Laplacian operators (Sec. 3.1 ) combined with the geodesic marching, we are able to perform a gradient descent to minimize criterion (5):

$$\Sigma_{t+1}(x) = \exp_{\Sigma_t(x)}(-\varepsilon \nabla C(\Sigma_t(x))) \quad (6)$$

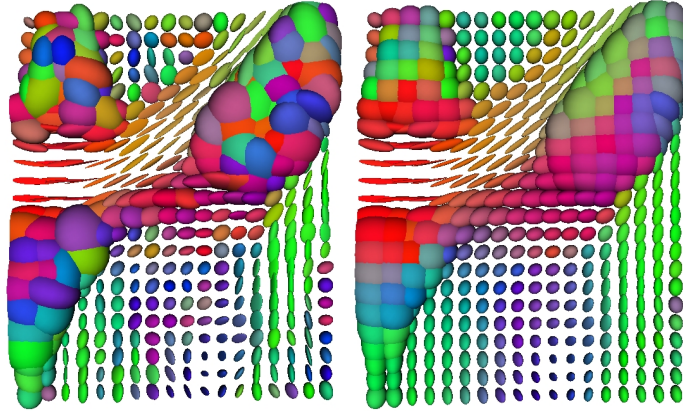


**Fig. 3. Anisotropic regularization of a slice of DTI.** Parameters:  $\kappa = 0.05$ ,  $\varepsilon = 0.1$ , iterations: 100 (diffusion time = 10). **Left:** Raw data. **Right:** Anisotropic filtering in the Riemannian framework. The boundary of the ventricles (region with large tensors) is well preserved. Remark that the left-right oriented tensors (in red) that are delineating a fiber tract are also conserved. The color code is the same as in Fig. 2.

Fig. 3 shows the effect of the anisotropic regularization on a slice of DTI. The parameters for the regularization are:  $\kappa = 0.05$ ,  $\varepsilon = 0.1$  and 100 iterations (total diffusion time: 10). The boundaries with the ventricles are conserved while the interior is correctly regularized. Moreover, at the top of the ventricles lies a fiber tract delimited with cigar-shaped tensors, which are also very well preserved.

## 4 Applications to Structure Tensor Images

The structure tensor has become a useful tool for the analysis of features in images. It is used in edges and corners detection [2], texture analysis [14, 15], filtering [16], and even medical image registration [17]. We show in this section how to apply our previously presented Riemannian framework to process structure tensor-valued images. In particular, we perform an anisotropic smoothing of the structure tensor field to enhance it, which could improve the quality of features detection.

### 4.1 The Structure Tensor

Let  $I$  be an image defined on a domain of  $\mathbb{R}^d$ . The structure tensor is based on the gradient of  $I$ :  $\nabla I = (\partial_1 I, \dots, \partial_d I)^T$ , where each directional derivative  $\partial_i I$  can be computed with a finite difference scheme or by filtering with a first order derivative of a Gaussian. The structure tensor  $S_\sigma$  can be defined as:

$$S_\sigma = G_\sigma * (\nabla I \nabla I^T)$$



with  $G_\sigma$  being a Gaussian of standard deviation  $\sigma$ . The variance  $\sigma$  controls the smoothness of the resulting tensor field. The noisier the image is, the higher  $\sigma$  must be to obtain a smooth field, but small structures may be wiped out. By contrast, smaller values of  $\sigma$  can help to extract low level features in images, but the resulting structure tensor image may be noisy. Consequently, one would like to perform an anisotropic filtering of the structure tensor field obtained with a low  $\sigma$ , in order to regularize homogeneous regions while preserving the boundaries with low-level features. In the following, we first compute the Riemannian gradient of a structure tensor image and compare it to the classical Euclidean gradient. Then, we perform an anisotropic filtering and discuss about the results.

## 4.2 Gradient of a Structure Tensor Image

Following the numerical scheme of Sec. 3.1, we computed the gradient norm of a structure tensor image obtained with a  $\sigma$  of 1.0 (Fig. 4 left is the original image). Then, we compared it to the Euclidean gradient. We also added noise in the original image to evaluate the robustness of both gradients. Results of comparisons are shown in Fig. 4.

First, we can notice that with the affine-invariant metric, outliers appear in the image background (Fig. 4 top right). This is intensified when adding noise (Fig. 4 bottom right): we see that the background is made with artefacts due to variations of small tensors that result from noise. Indeed, small tensors have as much importance as large ones because of the affine-invariance of the metric. Consequently, the Riemannian gradient of a variation of small tensors or large tensors will be identical. By contrast, the Euclidean gradient remains much less sensitive to tensors with small coefficients, and consequently only the main features are revealed (Fig. 4 bottom right and left).

Second, details that are not present in the Euclidean norm appear in the Riemannian gradient: this is the case, for example, of low-contrasted edges in the original image. This also results from the affine-invariance of the metric.

To conclude, the Riemannian framework can reveal lower structural information such as low contrasted edges but is highly sensitive to small variation in the tensor image, and thus suffers from a lack of robustness.

Let us now investigate how the anisotropic filtering scheme can restore the noisy structure tensor image.

## 4.3 Anisotropic Filtering of a Structure Tensor Image

We applied the anisotropic filtering scheme of Sec. 3.2 on the noisy structure tensor image of Fig. 4 bottom left. We used the following parameters:  $\kappa = 0.02$ ,  $\varepsilon = 0.1$  and 500 iterations (total diffusion time: 50). Results are presented in Fig. 5.

The affine-invariance causes the variations of small tensors to be highly contrasted in the norm of the Riemannian gradient and thus to be preserved during the filtering process. Figures 5 bottom illustrate this behavior: the top of the

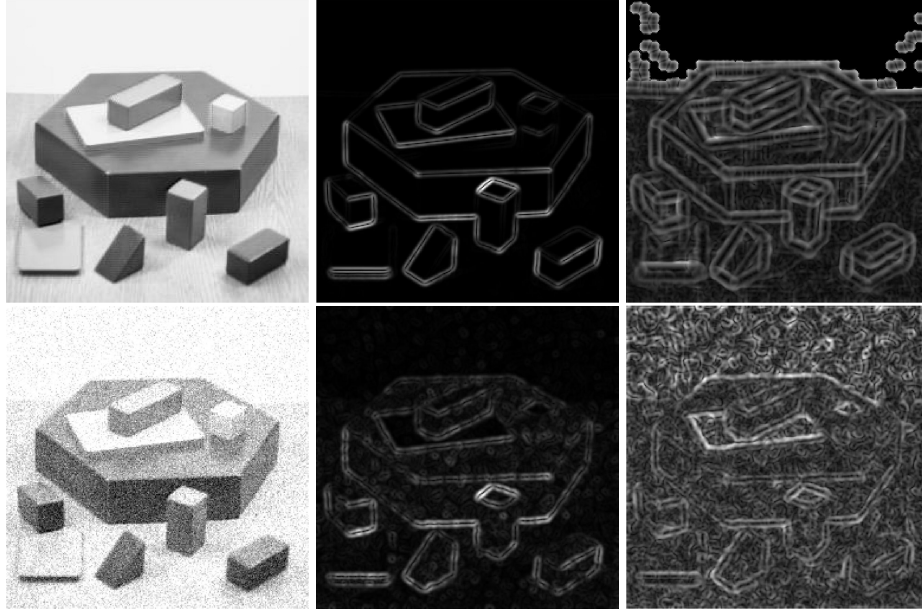


**Fig. 4. Euclidean gradient versus Riemannian gradient.** **Top row:** Original image (left), norm of the Euclidean (middle) and Riemannian (right) gradients. **Bottom row:** Noisy image (a Gaussian noise of variance 0.01 was added) (left), norm of the Euclidean (middle) and Riemannian (right) gradients.

original noisy image (middle image) is filled with artefacts that were preserved during the smoothing (right image). Taking the Euclidean norm (Fig. 5 top right) removes the artefacts in the image background. Homogeneous regions are smoother while edges are correctly conserved. However, some artefacts in the background that were expected to disappear are still present and the strength of most of the relevant edges is lower than in the affine-invariant case.

In conclusion, the affine-invariant metric that is well suited for DTI, or more generally for covariance matrices, seems not to be applicable directly to structure tensor images. The affine-invariance gives an identical role to small tensors versus large ones. Thus, while it allows to extract low-level features, it suffers from a lack of robustness.

However, the Riemannian framework we present in this paper is "parameterized" by the metric. The choice of the metric is crucial and determines the properties of the framework. The affine-invariance does not seem to be the best choice for structure tensor images, but a more adapted metric could significantly improve the results.

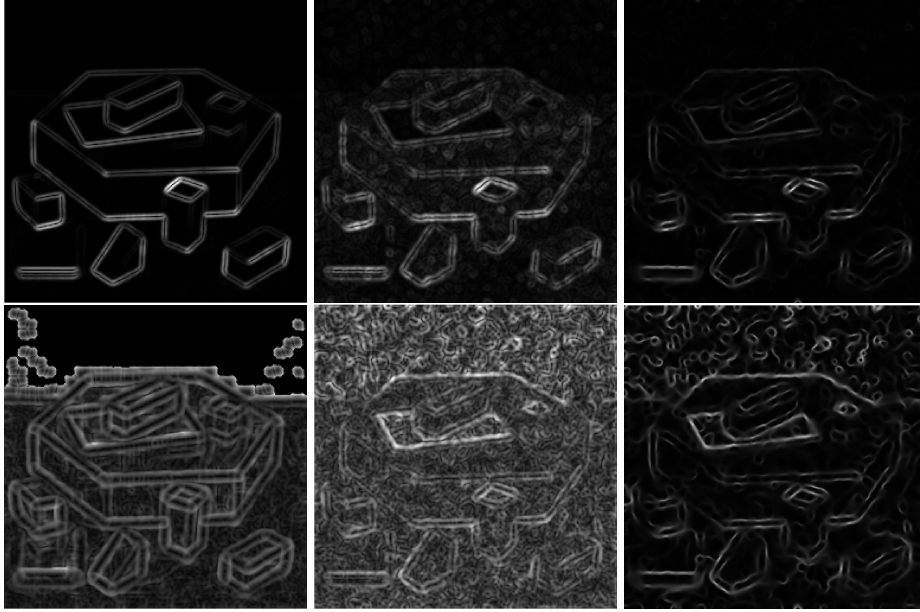


**Fig. 5. Anisotropic filtering of a noisy structure tensor image.** Diffusion parameters:  $\kappa = 0.02$ ,  $\varepsilon = 0.1$  and 500 iterations. **Top row:** From left to right: Original Euclidean gradient, Euclidean gradient with noise, Euclidean gradient after regularization. **Bottom row:** From left to right: Original Riemannian gradient, Riemannian gradient with noise, Riemannian gradient after regularization.

## 5 Discussion

We present in this paper a full Riemannian framework with an affine-invariant metric that allows to perform computations on tensors while insuring the result to be positive definite, which is often a critical issue as in DTI. While this framework is perfectly adapted to the processing of tensors representing covariance matrices, the affine-invariant metric does not appear to be the best suited choice for the processing of structure tensor images. In this case, the limitation comes from the affine-invariance which gives an identical influence to small and large tensors. Thus, an anisotropic smoothing will preserve the artefacts that are caused by variations of small tensors composing homogeneous regions. Beyond this limitation, the goal of this paper is to show that the choice of a Riemannian metric leads to a powerful framework which allows to extend classical vector space algorithms to manifolds thanks to the tools of differential geometry. One interesting track would be to specify what are the basic axioms that the structure tensor needs to satisfy and to derive the corresponding metric.

## References

1. P. Basser, J. Mattiello, and D. Le Bihan. MR diffusion tensor spectroscopy and imaging. *Biophysical Journal*, 66:259–267, 1994.
2. W. Förstner and E. Glüch. A fast operator for detection and precise location of distinct points, corners and centers of circular features. In *ISPRS*, pages 281–305. Interlaken, June 1987.
3. J. Bigün and G. H. Granlund. Optimal orientation detection of linear symmetry. In *First International Conference on Computer Vision*, pages 433–438. IEEE Computer Society Press, June 1987.
4. T. Brox, J. Weickert, B. Burgeth, and P. Mrázek. Nonlinear structure tensors. Technical report, Saarland University, October 2004.
5. O. Coulon, D. Alexander, and S. Arridge. Diffusion tensor magnetic resonance image regularization. *Medical Image Analysis*, 8(1):47–67, 2004.
6. D. Tschumperlé and R. Deriche. Orthonormal vector sets regularization with PDE's and applications. *Int. J. of Computer Vision (IJCV)*, 50(3):237–252, 2002.
7. P.T. Fletcher and S.C. Joshi. Principal geodesic analysis on symmetric spaces: Statistics of diffusion tensors. In *Proc. of CVAMIA and MMBIA Workshops, Prague, Czech Republic, May 15, 2004*, LNCS 3117, pages 87–98. Springer, 2004.
8. C. Lenglet, M. Rousson, R. Deriche, and O. Faugeras. Statistics on multivariate normal distributions: A geometric approach and its application to diffusion tensor MRI. Research Report 5242, INRIA, 2004.
9. P. Batchelor, M. Moakher, D. Atkinson, F. Calamante, and A. Connelly. A rigorous framework for diffusion tensor calculus. *Mag. Res. in Med.*, 53:221–225, 2005.
10. X. Pennec, P. Fillard, and N. Ayache. A Riemannian framework for tensor computing. *International Journal of Computer Vision*, 2005. To appear (accepted for publication).
11. X. Pennec. Probabilities and Statistics on Riemannian Manifolds: A Geometric approach. Research Report 5093, INRIA, January 2004. submitted to Int. Journal of Mathematical Imaging and Vision.
12. P. Perona and J. Malik. Scale-space and edge detection using anisotropic filtering. *IEEE Trans. Pattern Analysis and Machine Intelligence (PAMI)*, pages 629–639, 1990.
13. G. Aubert and P. Kornprobst. *Mathematical Problems in Image Processing*. Springer.
14. J. Bigün, G. H. Granlund, and J. Wiklund. Multidimensional orientation estimation with applications to texture analysis and optical flow. *IEEE Transactions on pattern Analysis and Machine Intelligence*, 13(8):775–790, August 1991.
15. A. R. Rao and B. G. Schunck. Computing oriented texture fields. *CVGIP: Graphical Models and Image Processing*, 53:157–185, 1991.
16. J. Weickert. Coherence-enhancing diffusion filtering. *IJCV*, 31(2/3):111–127, April 1999.
17. R. Stefanescu. *Parallel nonlinear registration of medical images with a priori information on anatomy and pathology*. PhD thesis, Nice-Sophia Antipolis University, 2005.